PNAS RESEARCH ARTICLE | NEUROSCIENCE OPEN ACCESS

# Spontaneous cortical dynamics from the first years to the golden years

Maggie P. Rempe[a,b,c,1], Lauren R. Ott[a,d,1], Giorgia Picci[a,c], Samantha H. Penhale[a], Nicholas J. Christopher-Hayes[a,e], Brandon J. Lew[a,b], Nathan M. Petro[a,c], Christine M. Embury[a], Mikki Schantell[a,b,c], Hallie J. Johnson[a], Hannah J. Okelberry[a], Kathryn L. Losh[a], Madelyn P. Willett[a], Rebecca A. Losh[a], Yu-Ping Wang[f], Vince D. Calhoun[g], Julia M. Stephen[h], Elizabeth Heinrichs-Graham[a,c,i], Max J. Kurz[a,c,i], and Tony W. Wilson[a,b,c,i,2]

Edited by Peter Strick, University of Pittsburgh Brain Institute, Pittsburgh, PA; received July 25, 2022; accepted November 8, 2022

**In the largest and most expansive lifespan magnetoencephalography (MEG) study to date (n = 434, 6 to 84 y), we provide critical data on the normative trajectory of resting-state spontaneous activity and its temporal dynamics. We perform cutting-edge analyses to examine age and sex effects on whole-brain, spatially-resolved relative and absolute power maps, and find significant age effects in all spectral bands in both types of maps. Specifically, lower frequencies showed a negative correlation with age, while higher frequencies positively correlated with age. These correlations were further probed with hierarchical regressions, which revealed significant nonlinear trajectories in key brain regions. Sex effects were found in absolute but not relative power maps, highlighting key differences between outcome indices that are generally used interchangeably. Our rigorous and innovative approach provides multispectral maps indicating the unique trajectory of spontaneous neural activity across the lifespan, and illuminates key methodological considerations with the widely used relative/absolute power maps of spontaneous cortical dynamics.**

oscillations | magnetoencephalography | aging | development | lifespan

## Significance

Resting-state neuroimaging techniques provide a unique opportunity to image the human brain in populations who may have difficulty performing cognitive tasks in the scanner. This includes clinical populations, young children, and older adults. In the largest MEG resting-state study to date, we address limitations in the current resting-state M/EEG literature, including the focus on narrow developmental windows, coarse spatial specificity, and limited use of absolute and relative power maps together, especially in spatially resolved electrophysiological studies. Our findings provide groundbreaking evidence that sex differences are often obscured by the use of relative versus absolute power maps and more broadly establish normative trajectories of the resting-state brain by illuminating age- and sex-related trends across the lifespan.

The advent of resting-state neuroimaging has provided a window into dynamic functional architectures underlying a myriad of processes, including brain development, aging, disease states, and psychopathology (1–10). Resting-state brain activity has been extensively captured and described using a range of neuroimaging techniques including functional MRI based on the blood oxygenation-level dependent signal, as well as methods examining the oscillatory dynamics of resting-state activity (i.e., spontaneous cortical activity), such as electroencephalography (EEG) and magnetoencephalography (MEG), which provide exquisite temporal resolution. A long history of resting-state studies utilizing EEG (for a brief review of EEG studies, see *SI Appendix*) have provided a solid foundation for more recent methodological advancements in resting-state electrophysiological imaging using MEG and EEG (11–13).

In addition to the high temporal resolution (~1 ms), MEG has excellent spatial precision (~3 to 5 mm), is noninvasive and silent, and provides reference-free measurements of electrical activity in active neural populations. These strengths make it an ideal modality for capturing developmental change in neuronal dynamics across a wide swath of the lifespan (14, 15). Using such imaging methods has yielded unique insights into how spontaneous oscillations within neuronal populations dynamically unfold. Thus far, many of these studies have focused on aberrant activity in pathological conditions such as Alzheimer's and Parkinson's disease (3, 5–7, 16, 17). Although several recent studies have shown remarkable shifts in the power of spontaneous cortical activity in healthy developmental and aging samples (18–20). Specifically, both the developing brain and the healthy aging brain seem to exhibit marked decreases in the lower canonical bands (i.e., delta, theta) along with increases in the higher frequencies (i.e., alpha, beta, gamma) (8–10, 13, 21–25).

A number of studies have examined developmentally focused effects of spontaneous cortical activity in populations ranging from childhood through adolescence, and into midadulthood. For example, in a sample of 9 to 15 y olds, Ott et al. found decreases in relative delta power with age and increases in relative alpha, beta, and gamma power with age during the transition from childhood to adolescence (26). Additionally, sex differences were observed in brain regions with protracted developmental trajectories across multiple frequency bands (i.e., delta, alpha, and beta) (26). In an earlier study that focused predominately on male participants from age 6 to 45 y, age-related increases in alpha power were detected in the temporal lobe, beta increases were seen in many brain regions, and gamma power increases were found primarily in the frontal lobe, while age-related decreases in theta were reported in the occipital lobe (27). These findings were largely confirmed

Author contributions: Y.-P.W., V.D.C., J.M.S., E.H.-G., M.J.K., and T.W.W. designed research; B.J.L., M.S., H.J.J., H.J.O., K.L.L., M.P.W., and R.A.L. performed research; M.P.R., L.R.O., G.P., S.H.P., N.J.C.-H., B.J.L., N.M.P., and C.M.E. contributed new reagents/analytic tools; M.P.R., L.R.O., G.P., and S.H.P. analyzed data; T.W.W. supervised research; T.W.W. reviewed the manuscript; T.W.W. edited the manuscript; and M.P.R., L.R.O., and G.P. wrote the paper.

The authors declare no competing interest.

This article is a PNAS Direct Submission.



[1]M.P.R. and L.R.O. contributed equally to this work.

[2]To whom correspondence may be addressed. Email: tony.wilson@boystown.org.

This article contains supporting information online at https://www.pnas.org/lookup/suppl/doi:10.1073/pnas.2212776120/-/DCSupplemental.

Published January 18, 2023.

in a subsample representing an even sex distribution, although the theta findings were less stable suggesting that theta may be more sexually dimorphic (27).

Other studies have focused on adult samples to identify aging effects in spontaneous neural dynamics. Hoshi and Shigihara examined age- and gender-specific characteristics in a sample of healthy adults aged 22 to 75 y and found that higher frequencies increased with age in anterior regions and decreased in posterior regions, while lower frequencies did not show a significant change with age (9). Additionally, sex differences were found in anterior regions of the brain such that males had stronger power in lower frequencies and females had stronger power in higher frequencies (9). However, using a larger age range (i.e., 7 to 84 y), another study found that spontaneous activity may follow a quadratic trajectory as opposed to a linear trend across the lifespan (8). Specifically, lower frequencies tended to decrease with age from childhood to adolescence while higher frequencies increased. However, around the sixth decade of life this trend switched directionality suggesting that relative power trends may not be linear across the whole lifespan (8). Of note, this study used whole-brain relative power values and did not perform source reconstruction, limiting spatial specificity.

While general developmental and aging patterns of low- and high-frequency bands have emerged, several methodological limitations have stymied greater progress in quantifying spontaneous cortical dynamics across the lifespan. As such, we sought to address three major pitfalls in the current resting-state MEG literature. First, previous studies examining age-related changes in spontaneous neural dynamics have typically focused on narrow developmental windows rather than examining the lifespan. In other words, most studies have focused on developmental populations or aging populations in isolation, with several investigations using binary approaches (e.g., young versus older adults). Second, studies that have examined a broader age range have been severely limited in their spatial specificity due to a lack of high-resolution source reconstruction. The few studies that performed source-level analyses have either focused on grossly defined regions of interest, collapsed across multiple brain regions, or the entire cortex. Third, prior MEG studies have tended to focus on relative power (i.e., power in one band relative to the total power across all bands) compared with absolute power maps. Although common in the EEG literature, absolute power maps are rarely utilized in MEG studies, despite the unique opportunity they afford researchers. Specifically, absolute power maps enable differences to be discerned in each band independently, without shifts in power within other bands influencing the results. The advantages of absolute power maps are further accentuated by the reference-free nature of MEG, which enables the strength of cortical currents to be directly estimated. Thus, at a minimum, absolute power maps provide critical information for correctly interpreting differences in relative power maps, although they may also provide novel information in their own right.

Thus, the current study was designed to address these major shortcomings. Critically, we maximize rigor and the spatiotemporal precision afforded by MEG using vertex-wise source level analyses in a large sample of participants (N = 434) ranging from 6 to 84 y of age to evaluate both relative and absolute power maps independently for age and sex effects across the lifespan. As noted above, MEG studies to date have generally focused on relative power maps as their outcome metric and broadly assumed that relative and absolute power maps could be used interchangeably, despite no definitive evidence supporting this. Thus, herein we probe this assumption using the largest sample to date, a single state-of-the-art MEG system, and advanced data analytics to systematically evaluate age- and sex-related changes in both relative and absolute spontaneous power across the lifespan.

## Results

A total of 434 participants (205 females) with an age range of 6 to 84 y (Mage = 25.13, SD = 20.51) were included in these analyses. Demographic characteristics are detailed in *SI Appendix*, Table S1, and the age distribution is shown in *SI Appendix*, Fig. S1. Of note, the age distribution of our sample was found to be skewed (skewness = 1.21). As such, all analyses were rerun using a random subsample in which age was not skewed (skewness = 0.91), which revealed an identical pattern of results.

Source imaging methods and processing followed the analysis pipeline outlined in Wiesman et al. (3). Using these source estimates, we then estimated the power of cortical activity in each of the canonical frequency bands: delta (2 to 4 Hz), theta (5 to 7 Hz), alpha (8 to 12 Hz), beta (15 to 29 Hz), and gamma (30 to 59 Hz; Fig. 1) to maximize comparability to previous studies.

### Linear Age Effects on Spontaneous Cortical Activity.

***Relative spontaneous cortical activity decreases in low frequencies and increases in high frequencies with age.*** Models of relative spontaneous power in the delta, theta, alpha, beta, and gamma frequency bands showed significant effects of age, when controlling for sex (Fig. 2). Specifically, relative delta power decreased with age across the entire cortex, with peak effects found in the bilateral middle temporal gyri (*Right*: $F(1,430) = 606.03$, $p_{FWE} < 0.001$; *Left*: $F(1,430) = 524.28$, $p_{FWE} < 0.001$; Fig. 2*A*). In addition, relative theta power decreased with age across temporoparietal cortices with peak effects found in the bilateral superior temporal gyri (*Right*: $F(1,430) = 75.30$, $p_{FWE} < 0.001$; *Left*: $F(1,430) = 101.66$, $p_{FWE} < 0.001$; Fig. 2*B*). In contrast, relative alpha power increased with age across the entire cortex, peaking in the bilateral inferior temporal gyri (*Right*: $F(1,430) = 337.03$, $p_{FWE} < 0.001$; *Left*: $F(1,430) = 382.67$, $p_{FWE} < 0.001$; Fig. 2*C*). Similarly, relative spontaneous beta power increased with age across the whole brain, with peak effects found in bilateral precentral gyri (*Right*: $F(1,430) = 785.73$, $p_{FWE} < 0.001$; *Left*: $F(1,430) = 795.63$, $p_{FWE} < 0.001$; Fig. 2*D*). Finally, relative spontaneous gamma power increased with age across the entire cortex, peaking in the bilateral superior frontal gyri (*Right*: $F(1,430) = 285.85$, $p_{FWE} < 0.001$; *Left*: $F(1,430) = 285.88$, $p_{FWE} < 0.001$; Fig. 2*E*).

***Absolute spontaneous cortical activity decreases in low frequencies and increases in high frequencies with age.*** To determine if age was associated with absolute power in a consistent manner and to eliminate the possibility that the age effects were primarily due to spectral shifts in power among the bands, we performed the same series of analyses testing age effects (controlling for sex) using absolute power spectral density (PSD) maps. Models of absolute spontaneous power in the delta, theta, alpha, beta, and gamma frequency bands showed significant effects of age, when controlling for sex (Fig. 3). Importantly, the spatial distribution of the absolute power findings overlapped almost entirely with those of the relative power maps, with the exception of delta. Specifically, absolute delta power decreased with age across the entire cortex, with peak effects found in the bilateral temporoparietal junctions (*Right*: $F(1,430) = 522.28$, $p_{FWE} < 0.001$; *Left*: $F(1,430) = 482.67$, $p_{FWE} < 0.001$; Fig. 3*A*). This contrasts with the relative maps, which showed a peak association in the middle temporal gyri. In addition, absolute theta power decreased with age across the cortex with a stronger relationship centered around the temporoparietal cortices, peaking in the right supramarginal gyrus and left superior temporal cortex (*Right*: $F(1,430) = 187.87$ $p_{FWE} < 0.001$; *Left*: $F(1,430) = 201.92$, $p_{FWE} < 0.001$; Fig. 3*B*). Conversely, absolute alpha power increased with age primarily in frontal and temporal cortices with peak effects in bilateral inferior temporal gyri (*Right*: $F(1,430) = 110.32$,

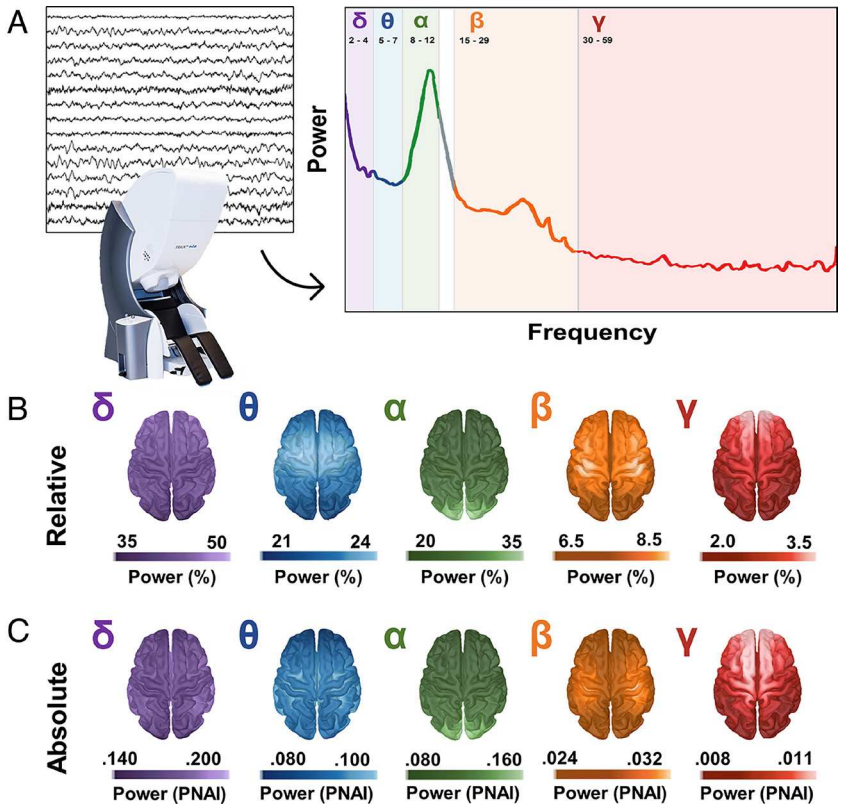


**Fig. 1.** Neural power distribution schematic. (*A*) Participants sat upright in the MEG with their eyes closed for 5 to 8 min. Individual sensors capture raw temporal dynamics as shown through the time series in the square box above the MEG. These magnetic field strength measurements can be projected to the cortex using source reconstruction approaches. Each location in these maps can be further broken down into individual canonical frequency bands as shown in the line graph to the right. Each frequency band is denoted by a specific color: delta (2 to 4 Hz) purple, theta (5 to 7 Hz) blue, alpha (8 to 12 Hz) green, beta (15 to 29 Hz) orange, and gamma (3 to 59 Hz) red. (*B*) Distribution of relative power. The grand-averaged distribution for relative power across all participants (n = 434) is shown for each of the frequencies denoted in part (*A*) in percentage units. Compared with the lower frequencies, higher frequency bands are comprised of a smaller percentage of relative power. Additionally, each band has a unique power distribution: delta-anterior frontal, theta-posterior frontal, alpha-occipital, beta-sensorimotor cortices, and gamma-prefrontal regions. (*C*) Distribution of absolute power. The grand-averaged distribution for absolute power across all participants (n = 434) is shown for each of the canonical frequency bands denoted in part (*A*) using the pseudo neural activity index (PNAI) as units. Each frequency band has a unique power distribution: delta-anterior frontotemporal, theta-temporal, alpha-occipital, beta-sensorimotor, and gamma-posterior frontal.



$p_{FWE} < 0.001$; *Left*: $F(1,430) = 115.58$, $p_{FWE} < 0.001$; Fig. 3*C*) and superior frontal gyri (*Right*: $F(1,430) = 38.05$, $p_{FWE} = 0.001$; *Left*: $F(1,430) = 38.33$, $p_{FWE} < 0.001$; Fig. 3*C*). Similarly, absolute spontaneous beta increased with age across the whole brain, with peak effects in bilateral precentral gyri (*Right*: $F(1,430) = 519.39$, $p_{FWE} < 0.001$; *Left*: $F(1,430) = 516.36$, $p_{FWE} < 0.001$; Fig. 3*D*). Finally, absolute spontaneous gamma power increased with age across the entire cortex, peaking in the bilateral superior frontal gyri (*Right*: $F(1,430) = 162.16$, $p_{FWE} < 0.001$; *Left*: $F(1,430) = 160.22$, $p_{FWE} < 0.001$; Fig. 3*E*).

### Quadratic Age Effects on Spontaneous Cortical Activity.

***Quadratic relationships between age and relative spontaneous cortical activity.*** Quadratic relationships of age and relative spontaneous cortical activity were tested using a hierarchical regression approach, using the peaks of each significant age effect as the input. Of note, each age effect showed peak effects in bilateral regions, so there was one peak per hemisphere in each regression model described here. Bonferroni correction was used to account for multiple comparisons ($p_{Bonferroni} < 0.05$ ($P = 0.05$/[5 spectral maps (delta, theta, alpha, beta, gamma) × 2 peaks (left and right) × 2 power normalizations (relative and absolute)] = 0.0025). The quadratic term significantly contributed to the model of relative spontaneous delta power in both right and left middle temporal gyri, indicating a quadratic relationship with age (*Right*: $R^2 = 0.78$, $F = 217.08$, $\Delta R^2 = 0.05$, $\Delta F = 58.55$, $P < 0.001$, $\beta = 1.07$, $b = 6.77 \times 10^{-5}$; *Left*: $R^2 = 0.79$, $\Delta F = 244.09$, $\Delta R^2 = 0.05$, $\Delta F = 54.96$, $P < 0.001$, $\beta = 1.00$, $b = 6.13 \times 10^{-5}$; Fig. 4*A*). In addition, the quadratic term significantly contributed to the model of relative spontaneous alpha power in both right and left inferior temporal gyri, again indicating a quadratic relationship with age (*Right*: $R^2 = 0.67$, $F = 118.01$, $\Delta R^2 = 0.02$, $\Delta F = 11.39$, $P < 0.001$, $\beta = -0.55$, $b = -3.12 \times 10^{-5}$; *Left*: $R^2 = 0.70$, $F = 134.17$, $\Delta R^2 = 0.01$, $\Delta F = 11.56$, $P = 0.001$, $\beta = -0.54$, $b = -3.08 \times 10^{-5}$; Fig. 4*C*). Relative spontaneous beta power in the right precentral gyrus also exhibited a quadratic relationship with age (*Right*: $R^2 = 0.81$, $F = 272.19$, $\Delta R^2 = 0.01$, $\Delta F = 11.20$, $P = 0.001$, $\beta = -0.44$, $b = -1.32 \times 10^{-5}$; Fig. 4*D*). Finally, relative spontaneous gamma power had a quadratic relationship with age in both right and left superior frontal gyri (*Right*: $R^2 = 0.71$, $F = 81.22$, $\Delta R^2 = 0.09$, $\Delta F = 81.22$, $P < 0.001$, $\beta = -1.41$, $b = -1.10 \times 10^{-5}$; *Left*: $R^2 = 0.72$, $F = 152.36$, $\Delta R^2 = 0.10$, $\Delta F = 92.01$, $P < 0.001$, $\beta = -1.48$, $b = -1.21 \times 10^{-5}$; Fig. 4*E*). None of the other peaks exhibited a quadratic relationship with age (Fig. 4).

***Quadratic relationships between age and absolute spontaneous cortical activity.*** The quadratic term significantly contributed to the model of absolute delta power in both right and left temporoparietal peaks, indicating a quadratic relationship with age (*Right*: $R^2 = 0.78$, $F = 217.73$, $\Delta R^2 = 0.08$, $\Delta F = 81.25$, $P < 0.001$, $\beta = 1.26$, $b = 4.94 \times 10^{-5}$; *Left*: $R^2 = 0.79$, $F = 230.92$, $\Delta R^2 = 0.07$, $\Delta F = 77.45$, $P < 0.001$, $\beta = 1.21$, $b = 4.74 \times 10^{-5}$; Fig. 4*F*). The quadratic term also significantly contributed to the model of absolute

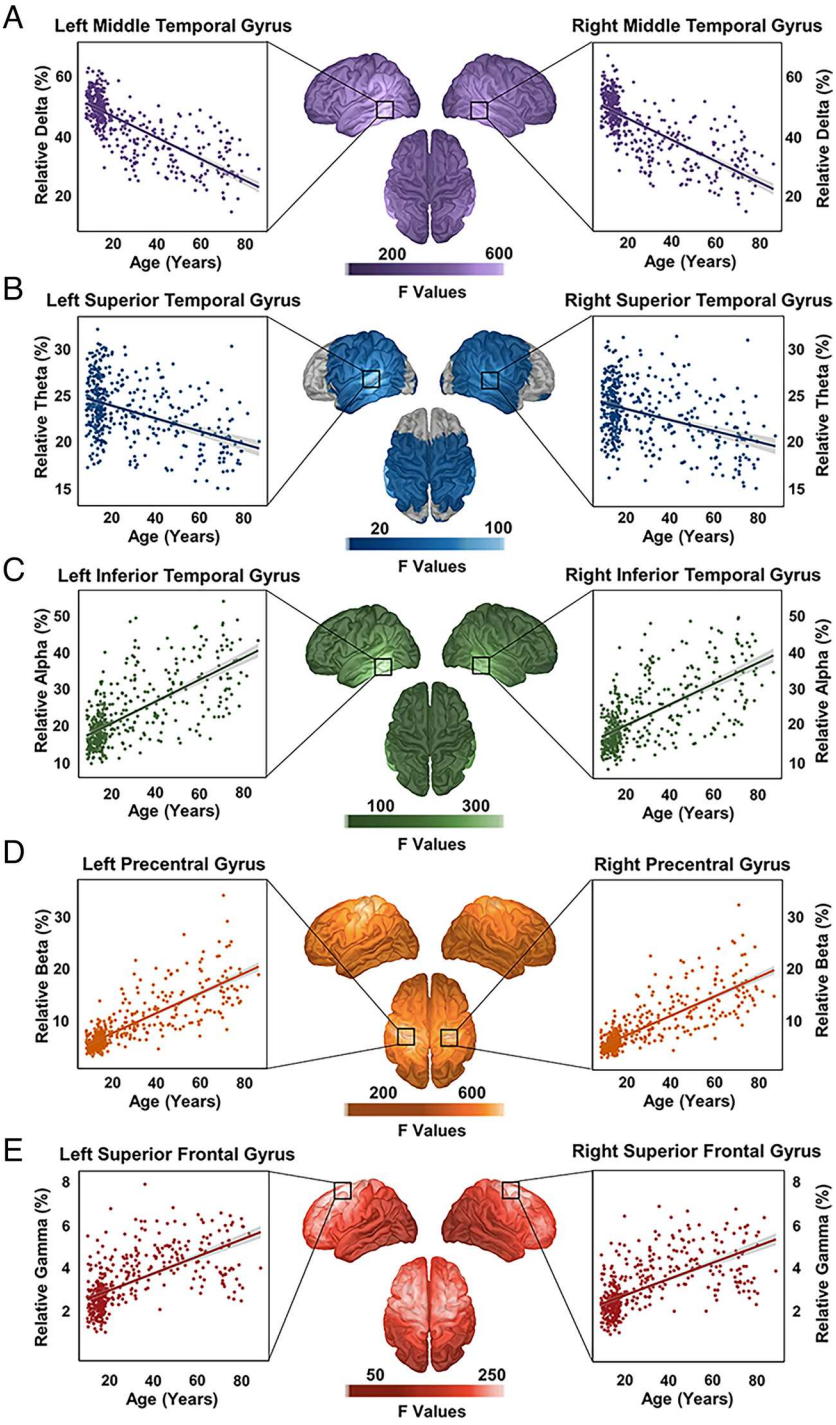


**Fig. 2.** The impact of age on relative power. (*Middle*) F-maps thresholded with TFCE are displayed for the main effect of age on relative power with the center of the black boxes denoting the peak for each respective hemisphere, although the box encompasses a much larger region than the peak vertex itself. The color bar beneath the brains shows the scale of F-values. Both the left and right clusters survived TFCE and FWE correction. (*Left* and *Right*) Scatterplots display the extracted values from the peak of the significant main effect of age on spontaneous relative power. Relative power (percent) is plotted on the Y-axis, and age (years) is plotted on the X-axis. The color distributions correspond to the canonical frequency band being shown (delta-purple, theta-blue, alpha-green, beta-orange, and gamma-red). The dots on the scatterplot represent each individual participant and the trendline represents the group's linear trajectory. (*A*) Delta (2 to 4 Hz): Relative power decreased with age across the cortex with peaks in bilateral middle temporal gyri. (*B*) Theta (5 to 7 Hz): Relative power decreased with age across the parietal and temporal lobes with peaks in bilateral superior temporal gyri. (*C*) Alpha (8 to 12 Hz): Relative power increased with age across the cortex with peaks in bilateral inferior temporal gyri. (*D*) Beta (15 to 29 Hz): Relative power increased with age across the cortex with peaks in bilateral precentral gyri. (*E*) Gamma (30 to 59 Hz): Relative power increased with age across the cortex with peaks in superior frontal gyri.

theta power, but only in the left superior temporal peak (*Left*: $R^2 = 0.58$, $F = 73.97$, $\Delta R^2 = 0.02$, $\Delta F = 10.53$, $P = 0.001$, $\beta = 0.59$, $b = 1.05 \times 10^{-5}$; Fig. 4*G*). In addition, the right precentral peak of absolute spontaneous beta power exhibited a quadratic relationship with age (*Right*: $R^2 = 0.74$, $F = 177.56$, $\Delta R^2 = 0.01$, $\Delta F = 5.29$, $P = 0.022$, $\beta = -0.34$, $b = -2.77 \times 10^{-6}$; Fig. 4*I*). Finally, absolute spontaneous gamma power had a quadratic relationship with age in both right and left superior frontal gyri (*Right*: $R^2 = 0.63$, $F = 95.59$, $\Delta R^2 = 0.12$, $\Delta F = 85.42$, $P < 0.001$, $\beta = -1.59$, $b = -2.45 \times 10^{-6}$; *Left*: $R^2 = 0.62$, $F = 89.29$, $\Delta R^2 = 0.10$, $\Delta F = 70.28$, $P < 0.001$, $\beta = -1.46$,

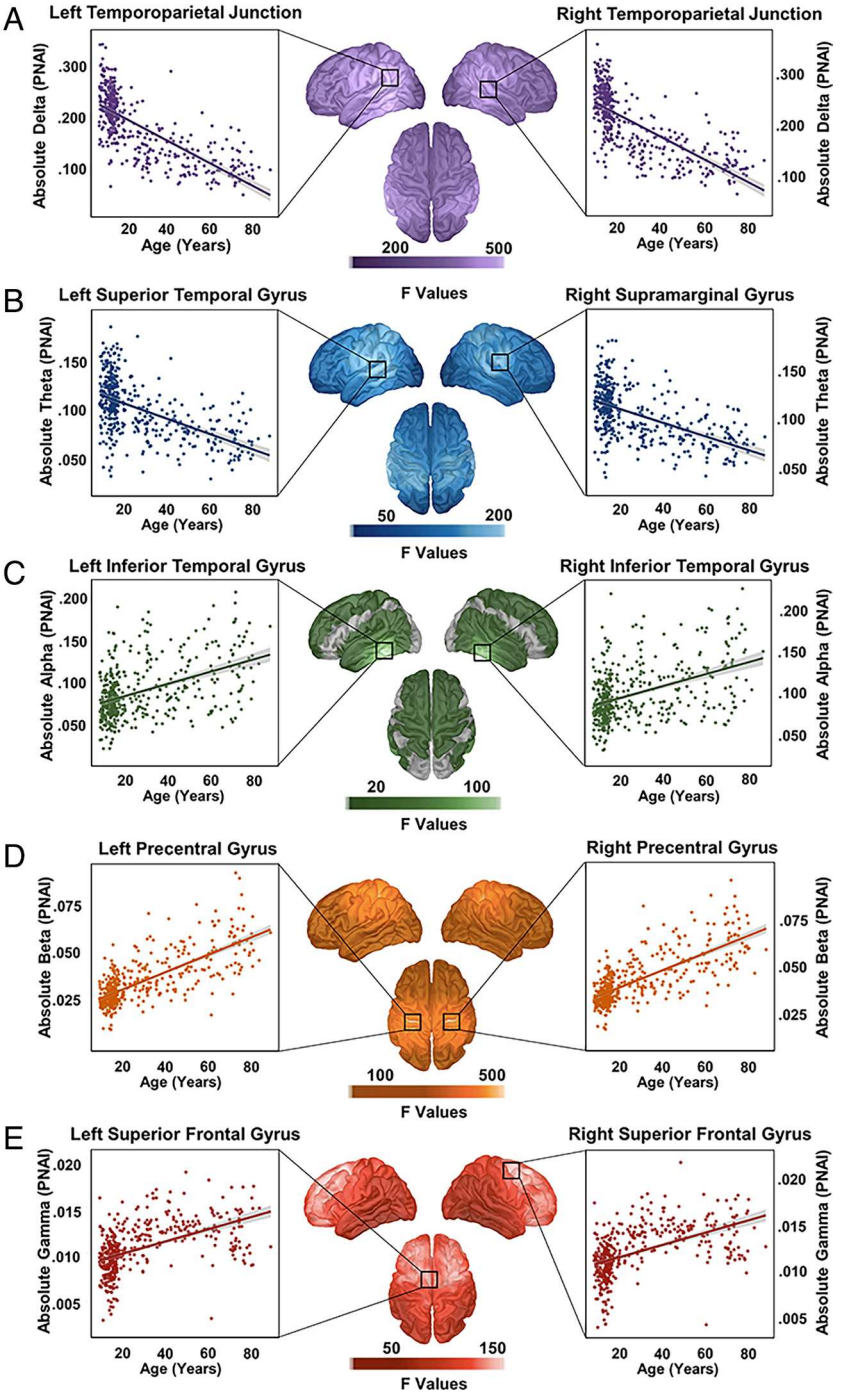


**Fig. 3.** The impact of age on absolute power. (*Middle*) F-maps thresholded with TFCE are displayed for the main effect of age on absolute power with the center of the black boxes denoting the peak for each respective hemisphere, although the box encompasses a much larger region than the peak vertex itself. The color bar beneath the brains shows the scale of F-values. Both the left and right clusters survived TFCE and FWE correction. (*Left* and *Right*) Scatterplots display the extracted values from the peak of the significant main effect of age on spontaneous absolute power. Absolute power, in units corresponding to the pseudo neural activity index (PNAI), is plotted on the Y-axis, and age (years) is plotted on the X-axis. The color distributions correspond to the canonical frequency band being shown (delta-purple, theta-blue, alpha-green, beta-orange, and gamma-red). The dots on the scatterplot represent each individual participant and the trendline represents the group's linear trajectory. (*A*) Delta (2 to 4 Hz). Absolute power decreased with age across the cortex with peaks in bilateral temporoparietal junction. (*B*) Theta (5 to 7 Hz). Absolute power decreased with age across the cortex with peaks in the left superior temporal gyrus and right supramarginal gyrus. (*C*) Alpha (8 to 12 Hz). Absolute power increased with age in frontal and temporal regions with peaks in bilateral inferior temporal gyri. (*D*) Beta (15 to 29 Hz). Absolute power increased with age across the cortex with peaks in bilateral precentral gyri. (*E*) Gamma (30 to 59 Hz). Absolute power increased with age across the cortex with peaks in superior frontal gyri.

$b = -2.38 \times 10^{-6}$; Fig. 4*J*). No other absolute power peaks exhibited a quadratic relationship with age.

### Sex Effects on Spontaneous Cortical Activity.

***Lifespan sex differences are absent in relative spontaneous cortical activity maps.*** No sex effects were identified in relative power maps. Of note, these models were performed using linear, nontransformed age as a covariate of no interest. Since significant linear relationships between age and power were found in all hemispheres and frequency bands, while significant nonlinear relationships were identified in only select hemispheres and frequency bands, linear models were used in order to take the

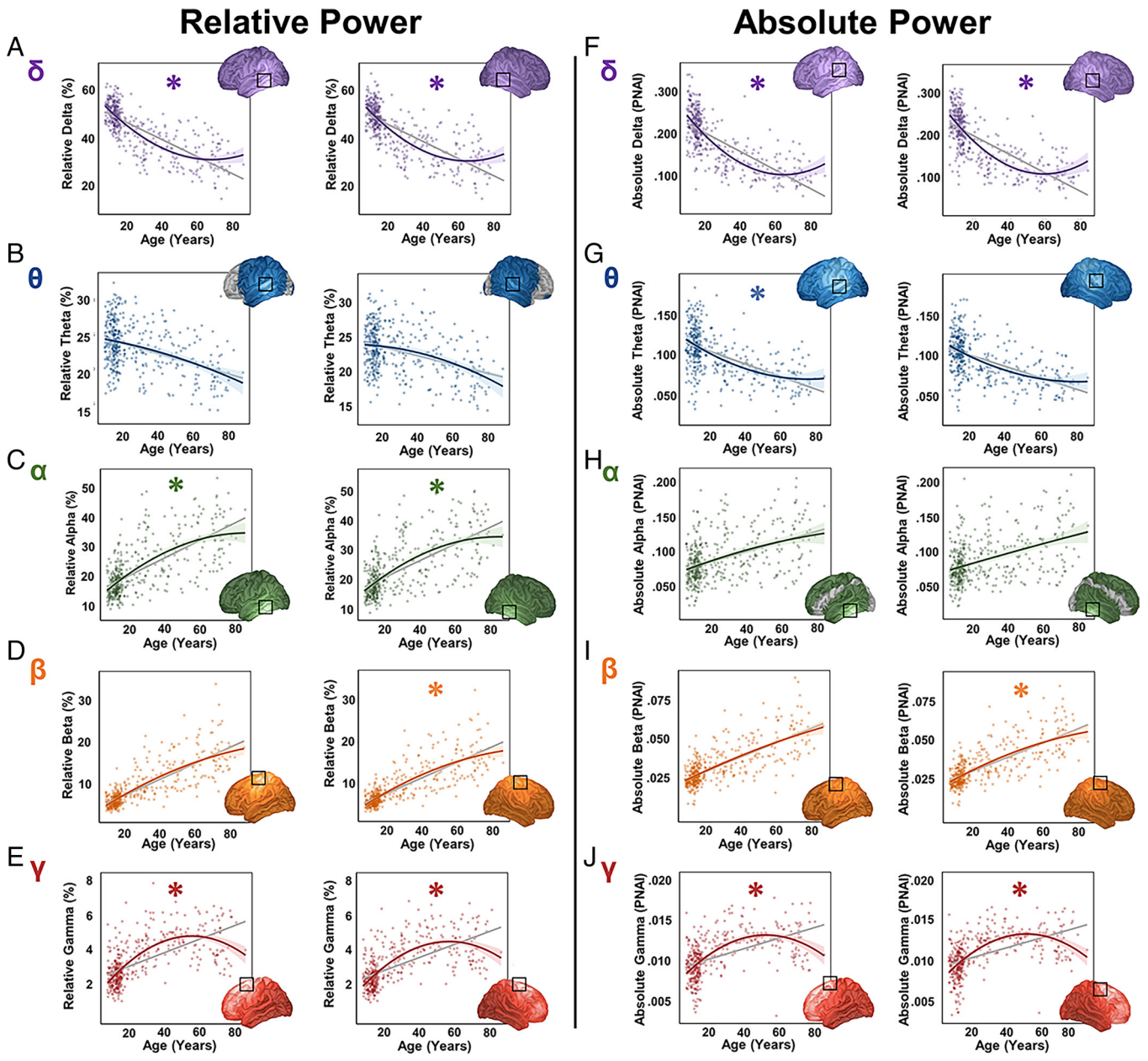


**Fig. 4.** Quadratic analysis of age effects. Scatterplots displaying the peak values of the significant main effect of age and power with linear (gray) and quadratic (color) fits for each significant age effect. Asterisks indicate that the quadratic fit is significantly better than the linear. The box on each brain represents the peak of each cluster from which data were extracted. The dots on the scatterplots represent each individual participant with the corresponding colored line showing the quadratic fit, with the shaded portion representing SE. The color distributions correspond to the canonical frequency band being shown (delta-purple, theta-blue, alpha-green, beta-orange, and gamma-red). (*Left*) Relative power (%) is plotted on the Y-axis, and age is plotted on the X-axis. Left hemispheric clusters are in the left column, and right hemispheric clusters are in the right column. (*Right*) Absolute power in pseudo neural activity index (PNAI) units is plotted on the Y-axis, and age is plotted on the X-axis. Left hemispheric clusters are in the left column and right hemispheric clusters are in the right column. (*A*) Delta (2 to 4 Hz): Relative delta power had a significant quadratic relationship with age in both right and left hemispheres. (*B*) Theta (5 to 7 Hz): Relative theta power did not have a significant quadratic relationship with age in either right or left hemisphere. (*C*) Alpha (8 to 12 Hz): Relative alpha power had a significant quadratic relationship with age in both right and left hemispheres. (*D*) Beta (15 to 29 Hz): Relative beta power had a significant quadratic relationship with age in the right but not the left hemisphere. (*E*) Gamma (30 to 59 Hz): Relative gamma power had a significant quadratic relationship with age in both right and left hemispheres. (*F*) Delta (2 to 4 Hz): Absolute delta power had a significant quadratic relationship with age in both right and left hemispheres. (*G*) Theta (5 to 7 Hz): Absolute theta power had a significant quadratic relationship with age in the left but not the right hemisphere. (*H*) Alpha (8 to 12 Hz): Absolute alpha power did not have a significant quadratic relationship with age in either right or left hemisphere. (*I*) Beta (15 to 29 Hz): Absolute beta power had a significant quadratic relationship with age in the right but not the left hemisphere. (*J*) Gamma (30 to 59 Hz): Absolute gamma power had a significant quadratic relationship with age in both right and left hemispheres.

same analytic approach for all frequency bands. Notably, no age by sex interactions were identified in relative power maps.

***Sex differences in absolute spontaneous cortical activity.*** Models of absolute delta, theta, and alpha power showed significant sex differences in multiple clusters, when controlling for age. As noted previously, linear age was used in these models. Specifically, absolute delta power primarily differed in frontoparietal cortices with peaks in bilateral frontal poles, such that males had higher absolute delta power than females (*Right*: $F(1,430) = 9.67$, $p_{FWE} = 0.010$; *Left*: $F(1,430) = 13.72$, $p_{FWE} = 0.001$; Fig. 5*A*). Similarly, absolute theta power differed in frontoparietal regions with peaks in bilateral superior frontal gyri, such that males had

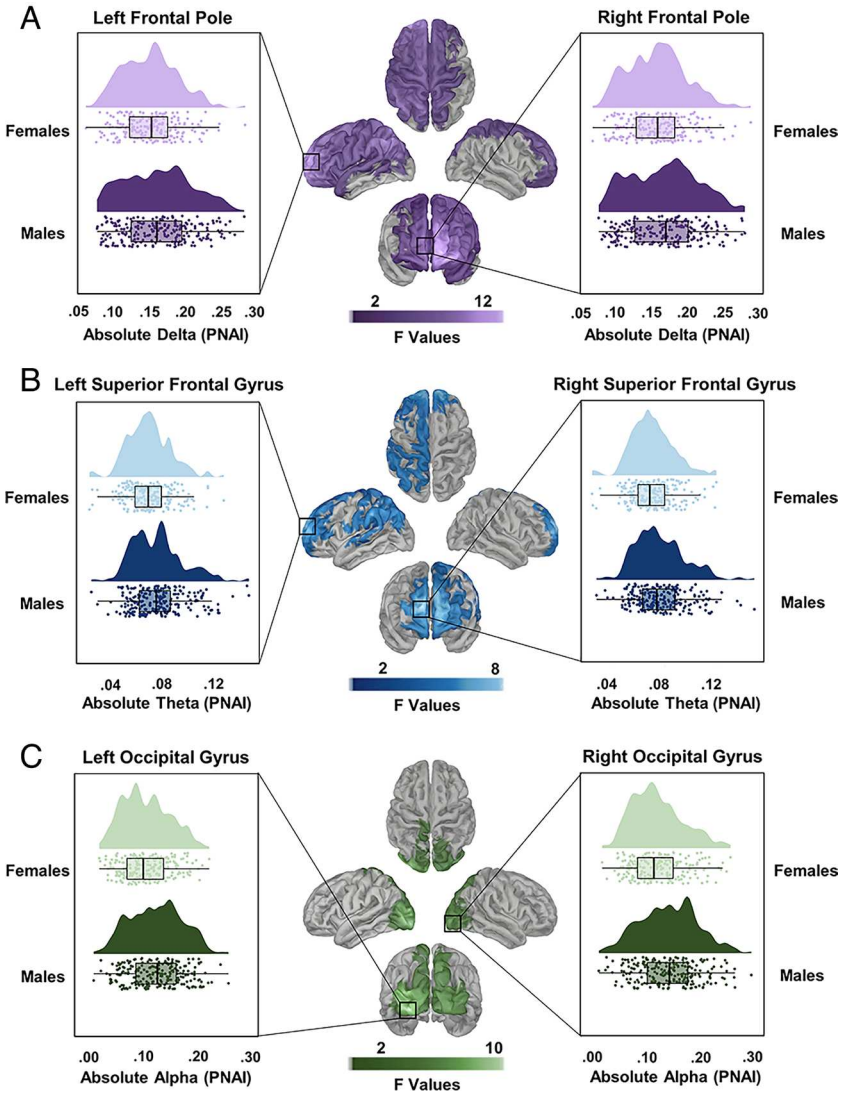


**Fig. 5.** The effect of sex on absolute power. (*Middle*) F-maps thresholded with TFCE are displayed for the main effect of sex on absolute power with the center of the black boxes denoting the peak for each respective hemisphere, although the box encompasses a much larger region than the peak vertex itself. The color bar beneath the brains shows the scale of F-values. Both the left and right clusters survived TFCE and FWE correction. (*Left* and *Right*) Scatterplots display the extracted values from the peak of the significant main effect of sex on spontaneous absolute power. Absolute power, in pseudo neural activity index (PNAI) units, is plotted on the X-axis, and sex is plotted on the Y-axis. The color distributions correspond to the canonical frequency band (delta-purple, theta-blue, alpha-green). The dots on the boxplots represent each individual participant with the raincloud representing the distribution. (*A*) Delta (2 to 4 Hz): Absolute power was increased in males relative to females across an extended area of the frontal lobe, with peaks at the frontal poles. (*B*) Theta (5 to 7 Hz): Absolute power was increased in males relative to females in a more restricted area of the anterior frontal lobe, with peaks at the frontal poles. (*C*) Alpha (8 to 12 Hz): Absolute power increased in males compared to females with peaks in lateral occipital lobes.

higher absolute theta power than females (*Right*: $F(1,430) = 8.41$, $p_{FWE} = 0.029$; *Left*: $F(1,430) = 7.34$, $p_{FWE} = 0.037$; Fig. 5*B*). Finally, absolute alpha power differed in occipital cortices with peaks in bilateral occipital gyri, such that males had higher absolute alpha power than females (*Right*: $F(1,430) = 7.80$, $p_{FWE} = 0.029$; *Left*: $F(1,430) = 10.27$, $p_{FWE} = 0.015$; Fig. 5*C*). No sex effects were identified in beta or gamma frequency bands. To ensure that quadratic relationships between power and age did not bias these results, we extracted power values from the peak of each cluster where a significant sex difference was identified and performed a *t* test including Age^2 as a nuisance covariate. Importantly, each of the sex effects remained significant ($P < 0.01$). Notably, no age by sex interactions were identified in absolute power maps.

## Discussion

In the largest lifespan MEG cohort to date, we sought to address three major pitfalls in the current resting-state MEG literature including, 1) the focus on narrow developmental windows rather than the lifespan, 2) coarse spatial specificity, and 3) the limited inquiry of absolute and relative power maps in the same study, particularly those that used source reconstruction and reported spatially resolved maps. Our comparison of absolute and relative spontaneous power demonstrated that although similar in many regards, sex differences only emerged in the absolute power maps. Of note, there are strengths and weaknesses in the use of either relative or absolute approaches to quantify spontaneous power across the cortex, which we discuss in turn below.

**Spatial Specificity of Age Effects.** The few studies examining broader age ranges have been limited in their spatial specificity, as they did not use high-resolution source reconstruction techniques that go beyond characterizations at the whole-cortex level or broadly defined regions of interest. Using vertex-wise source reconstruction and advanced data analytic techniques, we were able to capitalize on the superior spatial precision of

MEG and provide landmark evidence for specific cortical sources corresponding to the strongest age effects in each of the five canonical frequency bands (i.e., delta, theta, alpha, beta, and gamma) across the largest lifespan MEG cohort to date (6 to 84 y; N = 434).

Our findings demonstrating linear age-related changes in relative spontaneous cortical activity replicate and extend previous studies of developmental and aging populations. In particular, power decreases in lower frequencies (i.e., delta and theta) and increases in higher frequencies (i.e., alpha, beta, and gamma) are broadly consistent with existing EEG and MEG studies (8, 9, 11–13, 26, 27). Though we have replicated numerous previous studies showing age effects in spontaneous neural activity, we have added spatial information utilizing the advanced spatial precision afforded by MEG. Overall, our results showed similar locations for peaks of power between relative and absolute maps, with key differences found in the delta frequency band. Absolute delta power decreased with age across the entire cortex, with peak effects found in the bilateral temporoparietal junctions. This contrasts with the relative maps, which showed a peak association in the middle temporal gyrus. The temporoparietal junction is frequently associated with reorienting of attention and theory of mind (28, 29), while the middle temporal gyrus has been implicated in linguistic processing and the integration of auditory and visual processing streams (30–32). While the relation of delta waves to restoration and sleep is widely known, the task relevance of delta frequency oscillations remains less understood. However, a recent study reported processing speed abilities in a cognitively impaired older adult sample to be related to aberrations in resting-state delta oscillations in similar brain regions (i.e., middle temporal gyrus and temporoparietal junction) (3).

In contrast, peak locations between relative and absolute maps were similar in all other frequency bands. Specifically, theta power decreased with age across temporoparietal cortices with peak effects shown in perisylvian cortices, which are implicated in language processing, and more recently, social cognition (33, 34). Theta rhythms are most well-known for their involvement in memory, as they are the dominant rhythm in the hippocampus (35). Cortical theta oscillations have also been implicated in a wide variety of cognitive tasks, and are thought to support encoding or processing of new information (12). Alpha power increased with age across the entire cortex, peaking in the bilateral inferior temporal gyrus. Alpha frequency oscillations are the dominant rhythm in the occipital cortex and are tightly linked to visual perception, information processing, and attentional suppression (36–38). Relatedly, the inferior temporal gyrus is a key portion of the ventral visual pathway, which is crucial for object processing (39, 40). Additionally, beta power increased with age across the whole brain, with peak effects found in bilateral precentral gyri. This region, where beta is known to be the dominant rhythm, is highly associated with motor control (18, 19, 41). In fact, a few studies have linked this age-related increase in spontaneous beta activity to movement-associated beta oscillatory responses, and further motor performance (18, 19, 42). Finally, gamma power increased with age across the entire cortex, peaking in the bilateral superior frontal gyri including the supplemental motor area, which is responsible for motor planning and control (43). Gamma oscillations are also tightly related to sensory processing and integration, including that serving sensorimotor function (44, 45). Taken together, much of the regions which show the strongest age-related effects in each of the canonical frequency bands represent higher order cognitive processing, suggesting that these regions may be the most susceptible to developmental and aging processes.

Due to the wide age range in our sample, we sought to examine whether quadratic relationships may emerge and better explain patterns of spontaneous power observed with increasing chronological age. Interestingly, the majority of age-related effects were better explained by a quadratic rather than a linear curve and this frequently differed by both hemisphere and power metric (relative vs. absolute power). Of note, delta and gamma exhibited the most consistent pattern of findings with a quadratic fit explaining the relationship best in both hemispheres for both power measures. Specifically, delta decreased in power until about 60 y of age where power levels appeared to plateau before slightly increasing. The opposite was found in gamma, whereby an increase in power occurred until about 50 y of age where it then switched to a gradual decrease in power with chronological age. These findings largely agree with a previous aging study, which showed quadratic fits for delta, theta, alpha, high beta, and gamma frequency bands, though their analysis was limited to the sensor level and did not connect the findings to specific brain areas (8). The quadratic nature of these relationships suggests key age-related shifts in each spectral band, which may be indicative of normative aging processes. Understanding these processes is fundamental to characterizing spontaneous activity in healthy samples and will help in characterizing normative distributions that may support identifying altered developmental trajectories in disease states.

**Absolute Power Maps Show Sex Differences.** Notably, we also examined whether sex contributed to differences in spontaneous power. Once removing variance attributable to age, we found that males had greater absolute delta, theta, and alpha power compared with females. In regard to the alpha band, this study partially replicates a previous developmental MEG study showing a similar sex effect in the alpha frequency band (26), but also contradicts an aging study that showed stronger spontaneous alpha in females (9). Likewise, our delta findings (i.e., stronger in males) contradict both of these previous studies, as earlier work in typically developing youth (26) and healthy aging adults suggested stronger delta power in females compared with males. Neither of these studies found sex differences in theta activity. These discrepancies may be due to the restricted age ranges in prior studies, especially in the case of spontaneous alpha where prior work in youth versus adults had reached contradictory conclusions. However, the use of relative versus absolute power could also underlie these discrepancies, as no sex differences were observed in our relative power maps, suggesting that the sex effects observed in absolute power were likely obscured by changes in power within other frequency bands. This raises the concern that the sex effects reported in previous studies were driven by changes in other bands that then altered the overall proportion of power in alpha and delta. Potentially, we did not observe this in our relative power maps because of the larger sample size and/or the overall age range of our participant pool. The fact that the sex differences reported here would have gone undetected if relative power alone were used strongly supports the position that future studies should compute both types of maps to enhance rigor in their studies of spontaneous cortical activity in various populations.

**Differences in Relative and Absolute Power Maps.** Relative power, the more commonly reported measure, offers ease in interpretation as each frequency band is on the same percentage scale and enables broad changes in the overall distribution of power to be observed. However, as briefly alluded to above, the relative power approach is actually capturing the proportion of power in a specific frequency band and is assuming that the total amount of power across all frequency bands is uniform in the

population under study. Thus, estimates of relative power in a single canonical band can be strongly biased by changes in other frequency bands, as this would alter the overall distribution and lead to changes in the proportion even though the absolute power in the target band remained the same. In contrast, absolute power maps do not have the same interdependencies among the bands, but can be complicated to interpret because power levels vastly differ between bands due to the 1/f relationship. Additionally, intersubject variability is generally higher for absolute measures, and this may result in lower sensitivity to differences between groups and the relationship with age. Finally, in the context of EEG, absolute measures are slightly more difficult to interpret since the output measure is a difference between the target and reference electrodes, instead of a percent as with relative measures. MEG does not have this same concern since it is reference free.

The current study provides compelling evidence on the importance of examining both relative and absolute power. Notably, the age-related effects in each of the bands were seen in largely overlapping brain regions in both relative and absolute power maps, as both approaches identified similar peaks and overall cortical distributions. However, when testing the best fit trajectory for these effects, we showed that the age effects in many spectral bands were quadratic in nature and that these patterns varied between absolute and relative power. Likewise, sex differences were only identified in the absolute power maps, as estimates of relative power showed no effect of sex. Thus, these findings illuminate the importance of computing both absolute and relative power measures of spontaneous activity and suggest that assessing power changes in frequency bands relative to each other may obscure key differences. As such, we recommend that future MEG resting-state studies report both types of power maps to enhance rigor and reproducibility across studies.

**Limitations and Future Directions.** Some limitations of the current study must be acknowledged. First, though this study is comprised of a large sample with a wide age range, a longitudinal design (e.g., accelerated longitudinal) would enable researchers to map *individual* trajectories of spontaneous neural activity across the lifespan. Our cross-sectional design allowed us to look at a broad age range, but we were unable to examine person-specific trajectories from this design. Second, many of our participants were in the childhood to adolescence age range, and therefore the effects of pubertal hormones, irrespective of age, could be impactful in this sample (46). Finally, the present study was limited to examining differences in absolute and relative power as well as examining age- and sex-related associations with spontaneous neural dynamics. Future studies should expand on these analyses by examining how connectivity patterns change with age to gain a comprehensive understanding of how brain networks emerge and change throughout the healthy lifespan. Additionally, with the well-documented structural brain changes known to take place throughout life, future developmental studies should examine the correspondence between brain structure and spontaneous cortical activity and to what extent these metrics covary with age.

## Conclusion

The current study is the largest MEG study to date to investigate spontaneous neural dynamics across the lifespan (6 to 84 y). In this study, we addressed three major limitations in the current resting-state literature. In doing so, we independently replicated many of the known effects shown in previous research in a sample that extended across the lifespan, while identifying the precise brain regions where these dynamic changes were occurring. Our lifespan approach elucidated intriguing quadratic age effects across several frequencies, emphasizing the importance of fully characterizing the age spectrum rather than group-wise (i.e., old vs. young) or truncated comparisons. Additionally, we shed light on a major gap and limitation in the field such that when examining spontaneous cortical dynamics, it is necessary to examine both relative and absolute power maps to fully capture group differences and help guide interpretation. Our innovative approach not only highlighted many similarities between the power metrics, but it also illuminated notable, band-specific differences. Thus, because of these critical differences, we recommend that future resting-state studies report both absolute and relative power maps.

## Materials and Methods

**Participants.** 434 participants (205 females) between the ages of 6 and 84 y (Mage = 25.13, SD = 20.51) across five different studies were included in this analysis. Information regarding demographics and protocols of each study is summarized in *SI Appendix*, Table S1. Note that all five studies used the same MEG instrument. Adult participants were controls in studies examining neurological and psychiatric conditions, while pediatric participants were derived from normative studies of typical development. Further information establishing cognitive normality through neuropsychological assessment of the older adult sample is provided in the *SI Appendix*. Exclusionary criteria included inability to complete the full resting scan, any medical illness affecting the CNS, any neurological or psychiatric disorder, history of head trauma, current substance misuse, and standard MEG exclusion criteria (e.g., dental braces, metal implants, battery operated implants, and/or any type of ferromagnetic implanted material). All demographic data were reported by the participant or a guardian as a part of the intake process. For child participants, parents of the child participants signed informed consent forms, and child participants signed assent forms before proceeding with the study. For adult participants, written informed consent was obtained from each participant after a full description of the study. The local Institutional Review Board approved the study, and all protocols were in accordance with the Declaration of Helsinki.

**MEG Data Acquisition.** All MEG recordings took place in a one-layer magnetically shielded room (MSR) with active shielding engaged for environmental noise compensation. Participants were seated in a nonmagnetic chair within the MSR, with their head positioned within the sensor array. A 306-sensor MEGIN MEG system (Helsinki, Finland), equipped with 204 planar gradiometers and 102 magnetometers, was used to sample neuromagnetic responses continuously at 1 kHz with an acquisition bandwidth of 0.1 to 330 Hz. The same instrument was used across all recordings. Participants were instructed to rest with their eyes closed for 5 to 8 min and were monitored by a real-time audio–video feed from inside the shielded room throughout MEG data acquisition.

**Structural MRI Acquisition, Processing, and MEG-MRI Coregistration.** Prior to MEG acquisition, four coils were attached to the participants' heads and localized, together with the three fiducial points and scalp surface, using a 3-D digitizer (Fastrak 3SF0002, Polhemus Navigator Sciences, Colchester, VT, USA). Once the participant was positioned for MEG recording, an electrical current with a unique frequency label (e.g., 322 Hz) was fed to each of the coils. This induced a measurable magnetic field and allowed each coil to be localized in reference to the sensors throughout the recording session. Since coil locations were also known in head coordinates, all MEG measurements could be transformed into a common coordinate system. With this coordinate system (including the scalp surface points), each participant's MEG data were coregistered with their structural MRI prior to source space analyses using Brainstorm. For the 46 participants who did not have available T1 MRI data, age- and sex-matched MRIs were used to fit each participants' digitized head points (47).

**MEG Data Preprocessing.** Each MEG dataset was individually corrected for head motion and subjected to noise reduction using the signal space separation method with a temporal extension (MaxFilter v2.2; correlation limit: 0.950; correlation window duration: 6 s) (48). Noise-reduced MEG data underwent standard data preprocessing procedures using the Brainstorm software (49). A high-pass

filter of 1 Hz, low-pass filter of 200 Hz, and notch filters at 60 Hz and its harmonics were applied. Cardiac artifacts were identified in the raw MEG data and removed using an adaptive signal-space projection approach, which was subsequently accounted for during source reconstruction (50, 51). Data were then divided into 4-s epochs for detection and rejection of bad segments of data. Using custom lab software (https://github.com/nichrishayes/ArtifactScanTool), amplitude and gradient metrics for each epoch were computed, and epochs containing outlier values were rejected using an individualized fixed threshold method, supplemented with visual inspection. To account for variance across participants in distance between the brain and the MEG sensor array, as well as other sources of variance, we used an individually determined threshold based on the signal distribution for both amplitude and gradient to reject artifacts. Thirty epochs were removed from the end of each scan of our older adults to harmonize the length of their resting scan (*SI Appendix*) with the remaining dataset (52). Additionally, to account for environmental noise, we utilized empty room data to compute a noise covariance matrix for source imaging.

**MEG Source Imaging and Frequency Power Maps.** Source imaging methods and processing largely followed the analysis pipeline outlined in Wiesman et al. (3). Source analysis of neuromagnetic fields used an overlapping-spheres forward model, unconstrained to the cortical surface. This approach models a single sphere per each sensor, which in this study included 204 gradiometers (minus any channels previously marked as "bad") for each participant. A linearly constrained minimum variance beamformer implemented in Brainstorm (49) was used to spatially filter the epoched data based on the data covariance computed from the resting-state recording. Using these source estimates, we then estimated the power of cortical activity in each of five canonical frequency bands: delta (2 to 4 Hz), theta (5 to 7 Hz), alpha (8 to 12 Hz), beta (15 to 29 Hz), and gamma (30 to 59 Hz). We focused on these five canonical frequency bands (Fig. 1) to maximize comparability to previous studies. Neural oscillations in each of these spectral windows have been implicated in a wide range of cognitive processes. Delta oscillations have been commonly associated with inhibition of sensory processing during internal concentration (53). Theta oscillations have been linked to many cognitive processes and, most notably, are the dominant rhythm found in the hippocampus, supporting its involvement in memory (35). Alpha activity is often attributed to attentional suppression; for example, alpha amplitude increases when objects need to be ignored or when one's eyes are closed (36, 37). Beta oscillations have been well documented in motor processing and are the dominant frequency in sensorimotor cortices (18, 19, 41). Finally, gamma oscillations are thought to relate to sensory perception and integration (44).

We used Welch's method for estimating power spectrum densities (PSD) per 4-s epoch across each MEG recording, with one-second sliding Hamming windows overlapping at 50%. From here, two sets of PSD maps were created. To create nonnormalized maps, these raw PSD maps were averaged across epochs to obtain one absolute PSD map per participant. The units in these absolute maps correspond to the pseudo neural activity index (PNAI), which is a modified version of Van Veen's neural activity index (54). In addition, to create relative maps, we standardized the raw PSD values of each epoch at each frequency bin to the total power across the frequency spectrum, thus these maps are measured in percentages. For each participant, we then averaged PSD maps across epochs to obtain one relative PSD map per participant. Finally, the norm of the three unconstrained orientations per location were then projected onto a common FSAverage template surface separately for the absolute and relative maps, and these were used for further statistical analysis.

**Statistical Analysis and Visualization.** Whole-brain PSD maps per canonical band were analyzed in SPM12 to examine spatially specific effects of age and sex, and their interactions. For each frequency band, we ran an ANCOVA with age as a continuous predictor and sex as a categorical predictor and modeled the respective interaction term. To account for nonuniform spatial autocorrelation in the data, avoid assumptions of parametric modeling, and avoid selecting arbitrary cluster-forming thresholds, threshold-free cluster enhancement [TFCE; E = 1.0, H = 2.0; 5,000 permutations (55)] was performed, with multiple comparisons correction set to cluster-wise pFWE <0.05. Finally, F-maps were thresholded by utilizing the clusters that survived correction. Of note, these analyses were performed for each relative and absolute whole-brain PSD maps. Data from peak vertices were used to display the corresponding effects using ggplot2 (56).

**Quadratic Relationships between Age and Spontaneous Cortical Activity.** Quadratic relationships were tested using a hierarchical regression approach. For this, spontaneous power values were extracted from the peak of each cluster representing significant age effects. In the first step of the hierarchical regression, age and sex were entered, followed by the quadratic age term in the second step. This was performed for each frequency band in which significant age effects were identified in relative and absolute PSD maps.

**Data, Materials, and Software Availability.** MEG recordings from each participant (.fif), structural MRI data (.nii), and age/sex (.xlsx) data have been deposited in the institutional website of Boys Town National Research Hospital (https://cdn.boystown.org/media/Rempe_Ott_PNAS_2023_Data.zip).

**ACKNOWLEDGMENTS.** This research was supported by grants R01-MH121101, R01-MH116782, R01-DA047828, R01-MH118013, RF1-MH117032, R01--DA056223, R01-MH123610, R01-HD086245, F30-DA048713, F31-DA056296, and P20-GM144641 from the NIH, and grants #1539067 and #2112455 from the NSF. The funders had no role in study design, data collection, analysis, decision to publish, or manuscript preparation. We want to thank the participants for volunteering to participate in the study and our staff and local collaborators for contributing to the work. We would also like to specifically thank Nichole Knott for extensive help with the MEG recordings.

Author affiliations: [a]Institute for Human Neuroscience, Boys Town National Research Hospital, Boys Town, NE 68010; [b]College of Medicine, University of Nebraska Medical Center, Omaha, NE 68198; [c]Center for Pediatric Brain Health, Boys Town National Research Hospital, Boys Town, NE 68010; [d]San Diego State University/University of California San Diego Joint Doctoral Program in Clinical Psychology, San Diego, CA 92120; [e]Center for Mind and Brain, University of California–Davis, Davis, CA 95618; [f]Department of Biomedical Engineering, Tulane University, New Orleans, LA 70118; [g]Tri-institutional Center for Translational Research in Neuroimaging and Data Science, Georgia State University, Georgia Institute of Technology, and Emory University, Atlanta, GA 30303; [h]Mind Research Network, Albuquerque, NM 87106; and [i]Department of Pharmacology & Neuroscience, Creighton University, Omaha, NE 68178

1. J. C. Edgar *et al.*, Resting-state alpha in autism spectrum disorder and alpha associations with thalamic volume. *J. Autism Dev. Disord.* **45**, 795–804 (2015).
2. A. K. Engel, P. Fries, Beta-band oscillations–signalling the status quo? *Curr. Opin. Neurobiol.* **20**, 156–165 (2010).
3. A. I. Wiesman *et al.*, Spatio-spectral relationships between pathological neural dynamics and cognitive impairment along the Alzheimer's disease spectrum. *Alzheimers Dement. (Amst)* **13**, e12200 (2021).
4. A. I. Wiesman, Aberrant neurophysiological signaling underlies speech impairments in Parkinson's disease. medRxiv [Preprint] (2022). https://doi.org/10.1101/2022.04.01.22273315. (Accessed 19 April 2022).
5. J. Bosboom *et al.*, Resting state oscillatory brain dynamics in Parkinson's disease: An MEG study. *Clin. Neurophysiol.* **117**, 2521–2531 (2006).
6. J. Bosboom, D. Stoffers, E. C. Wolters, C. J. Stam, H. W. Berendse, MEG resting state functional connectivity in Parkinson's disease related dementia. *J. Neural Trans.* **116**, 193–202 (2009).
7. K. T. O. Dubbelink *et al.*, Resting-state functional connectivity as a marker of disease progression in Parkinson's disease: A longitudinal MEG study. *Neuroimage Clin.* **2**, 612–619 (2013).
8. C. Gómez, J. M. Pérez-Macías, J. Poza, A. Fernández, R. Hornero, Spectral changes in spontaneous MEG activity across the lifespan. *J. Neural Eng.* **10**, 066006 (2013).
9. H. Hoshi, Y. Shigihara, Age-and gender-specific characteristics of the resting-state brain activity: A magnetoencephalography study. *Aging (Albany NY)* **12**, 21613 (2020).
10. R. J. Barry, A. R. Clarke, Spontaneous EEG oscillations in children, adolescents, and adults: Typical development, and pathological aspects in relation to AD/HD. *J. Psychophysiol.* **23**, 157–173 (2009).
11. C. Babiloni *et al.*, Sources of cortical rhythms in adults during physiological aging: A multicentric EEG study. *Hum. Brain Mapp.* **27**, 162–172 (2006).
12. W. Klimesch, EEG alpha and theta oscillations reflect cognitive and memory performance: A review and analysis. *Brain Res. Rev.* **29**, 169–195 (1999).
13. O. Vysata, J. Kukal, A. Prochazka, L. Pazdera, M. Valis, Age-related changes in the energy and spectral composition of EEG. *Neurophysiology* **44**, 63–67 (2012).
14. S. Baillet, Magnetoencephalography for brain electrophysiology and imaging. *Nat. Neurosci.* **20**, 327–339 (2017).
15. T. W. Wilson, E. Heinrichs-Graham, A. L. Proskovec, T. J. McDermott, Neuroimaging with magnetoencephalography: A dynamic view of brain pathophysiology. *Trans. Res.* **175**, 17–36 (2016).
16. M. Engels *et al.*, Alzheimer's disease: The state of the art in resting-state magnetoencephalography. *Clin. Neurophysiol.* **128**, 1426–1437 (2017).
17. A. I. Wiesman *et al.*, Spatially resolved neural slowing predicts impairment and amyloid burden in Alzheimer's disease. *Brain* **145**, 2177–2189 (2022).
18. E. Heinrichs-Graham, T. W. Wilson, Is an absolute level of cortical beta suppression required for proper movement? Magnetoencephalographic evidence from healthy aging. *Neuroimage* **134**, 514–521 (2016).

19. E. Heinrichs-Graham *et al.*, The lifespan trajectory of neural oscillatory activity in the motor system. *Dev. Cogn. Neurosci.* **30**, 159–168 (2018).
20. H. E. Rossiter, E. M. Davis, E. V. Clark, M.-H. Boudrias, N. S. Ward, Beta oscillations reflect changes in motor cortex inhibition in healthy ageing. *Neuroimage* **91**, 360–365 (2014).
21. L. Michels *et al.*, Developmental changes of functional and directed resting-state connectivities associated with neuronal oscillations in EEG. *Neuroimage* **81**, 231–242 (2013).
22. S. J. Segalowitz, D. L. Santesso, M. K. Jetha, Electrophysiological changes during adolescence: A review. *Brain Cogn.* **72**, 86–100 (2010).
23. P. J. Uhlhaas, F. Roux, E. Rodriguez, A. Rotarska-Jagiela, W. Singer, Neural synchrony and the development of cortical networks. *Trends Cogn. Sci.* **14**, 72–80 (2010).
24. R. J. Barry, F. M. De Blasio, EEG differences between eyes-closed and eyes-open resting remain in healthy ageing. *Biol. Psychol.* **129**, 293–304 (2017).
25. R. Ishii *et al.*, Healthy and pathological brain aging: From the perspective of oscillations, functional connectivity, and signal complexity. *Neuropsychobiology* **75**, 151–161 (2017).
26. L. R. Ott *et al.*, Spontaneous cortical MEG activity undergoes unique age- and sex-related changes during the transition to adolescence. *Neuroimage* **244**, 118552 (2021).
27. B. A. E. Hunt *et al.*, Spatial and spectral trajectories in typical neurodevelopment from childhood to middle age. *Netw. Neurosci.* **3**, 497–520 (2019).
28. R. Saxe, N. Kanwisher, People thinking about thinking people: The role of the temporo-parietal junction in 'theory of mind' in *Social Neuroscience*, (Psychology Press, 2013), pp. 171–182.
29. S. C. Krall *et al.*, The role of the right temporoparietal junction in attention and social interaction as revealed by ALE meta-analysis. *Brain Struct. Funct.* **220**, 587–604 (2015).
30. J. R. Binder, R. H. Desai, W. W. Graves, L. L. Conant, Where is the semantic system? A critical review and meta-analysis of 120 functional neuroimaging studies. *Cereb. Cortex* **19**, 2767–2796 (2009).
31. L. Papeo, B. Agostini, A. Lingnau, The large-scale organization of gestures and words in the middle temporal gyrus. *J. Neurosci.* **39**, 5966–5974 (2019).
32. J. Xu *et al.*, Delineating functional segregations of the human middle temporal gyrus with resting-state functional connectivity and coactivation patterns. *Hum. Brain Mapp.* **40**, 5159–5171 (2019).
33. N. Mesgarani, C. Cheung, K. Johnson, E. F. Chang, Phonetic feature encoding in human superior temporal gyrus. *Science* **343**, 1006–1010 (2014).
34. R. Adolphs, Cognitive neuroscience of human social behaviour. *Nat. Rev. Neurosci.* **4**, 165–178 (2003).
35. G. Buzsáki, Theta oscillations in the hippocampus. *Neuron* **33**, 325–340 (2002).
36. W. Klimesch, Alpha-band oscillations, attention, and controlled access to stored information. *Trends Cogn. Sci.* **16**, 606–617 (2012).
37. J. J. Foxe, A. C. Snyder, The role of alpha-band brain oscillations as a sensory suppression mechanism during selective attention. *Front. Psychol.* **2**, 154 (2011).
38. A. I. Wiesman, E. Heinrichs-Graham, A. L. Proskovec, T. J. McDermott, T. W. Wilson, Oscillations during observations: Dynamic oscillatory networks serving visuospatial attention. *Hum. Brain Mapp.* **38**, 5128–5140 (2017).
39. A. Ishai, L. G. Ungerleider, A. Martin, J. L. Schouten, J. V. Haxby, Distributed representation of objects in the human ventral visual pathway. *Proc. Natl. Acad. Sci. U.S.A.* **96**, 9379–9384 (1999).
40. N. K. Logothetis, D. L. Sheinberg, Visual object recognition. *Annu. Rev. Neurosci.* **19**, 577–621 (1996).
41. N. J. Davis, S. P. Tomlinson, H. M. Morgan, The role of beta-frequency neural oscillations in motor control. *J. Neurosci.* **32**, 403–404 (2012).
42. M. P. Rempe *et al.*, Spontaneous sensorimotor beta power and cortical thickness uniquely predict motor function in healthy aging. *Neuroimage* **263**, 119651 (2022).
43. R. P. Dum, Frontal lobe inputs to the digit representations of the motor areas on the lateral surface of the Hemisphere. *J. Neurosci.* **25**, 1375–1386 (2005).
44. D. L. Pritchett, J. H. Siegle, C. A. Deister, C. I. Moore, For things needing your attention: The role of neocortical gamma in sensory perception. *Curr. Opin. Neurobiol.* **31**, 254–263 (2015).
45. R. K. Spooner, A. I. Wiesman, A. L. Proskovec, E. Heinrichs-Graham, T. W. Wilson, Rhythmic spontaneous activity mediates the age-related decline in somatosensory function. *Cereb. Cortex* **29**, 680–688 (2019).
46. S. H. Penhale *et al.*, Impacts of adrenarcheal DHEA levels on spontaneous cortical activity during development. *Dev. Cogn. Neurosci.* **57**, 101153 (2022).
47. A. I. Wiesman, T. W. Wilson, Alpha frequency entrainment reduces the effect of visual distractors. *J. cogn. Neurosci.* **31**, 1392–1403 (2019).
48. S. Taulu, J. Simola, Spatiotemporal signal space separation method for rejecting nearby interference in MEG measurements. *Phys. Med. Biol.* **51**, 1759–1768 (2006).
49. F. Tadel, S. Baillet, J. C. Mosher, D. Pantazis, R. M. Leahy, Brainstorm: A user-friendly application for MEG/EEG analysis. *Comput. Intell. Neurosci.* **2011**, 879716 (2011).
50. M. A. Uusitalo, R. J. Ilmoniemi, Signal-space projection method for separating MEG or EEG into components. *Med. Biol. Eng. Comput.* **35**, 135–140 (1997).
51. N. Ille, P. Berg, M. Scherg, Artifact correction of the ongoing EEG using spatial filters based on artifact and brain signal topographies. *J. Clin. Neurophysiol.* **19**, 113–124 (2002).
52. A. I. Wiesman, J. da Silva Castanheira, S. Baillet, Stability of spectral estimates in resting-state magnetoencephalography: Recommendations for minimal data duration with neuroanatomical specificity. *Neuroimage* **247**, 118823 (2022).
53. T. Harmony, The functional significance of delta oscillations in cognitive processing. *Front. Integr. Neurosci.* **7**, 83 (2013).
54. S. Robinson, Localization of event-related activity by SAM (erf). *Neurol. Clin. Neurophysiol.* **2004**, 109 (2004).
55. S. M. Smith, T. E. Nichols, Threshold-free cluster enhancement: Addressing problems of smoothing, threshold dependence and localisation in cluster inference. *Neuroimage* **44**, 83–98 (2009).
56. H. Wickham, *ggplot2: Elegant Graphics for Data Analysis* (Springer, 2016).